PCCP

Towards electrochemical purification of chemically reduced graphene oxide from redox accessible impurities

Journal:	*Physical Chemistry Chemical Physics*
Manuscript ID:	CP-ART-01-2014-000371.R1
Article Type:	Paper
Date Submitted by the Author:	13-Feb-2014

Complete List of Authors:	Tan, Shu Min; Nanyang Technological University, Division of Chemistry and Biological Chemistry Ambrosi, Adriano; Nanyang Technological University, Chemistry and Biological Chemistry Khezri, Bahareh; Nanyang Technological University, School of Physical and Mathematical Sciences Webster, Richard; Nanyang Technological University, Division of Chemistry and Biological Chemistry Pumera, Martin; Nanyang Technological University, Chemistry and Biological Chemistry

Journal Name

RSCPublishing

ARTICLE

Towards electrochemical purification of chemically reduced graphene oxide from redox accessible impurities

Cite this: DOI: 10.1039/x0xx00000x

Shu Min Tan, Adriano Ambrosi, Bahareh Khezri, Richard D. Webster and Martin Pumera*[a]

Received ooth January 2012,
Accepted ooth January 2012

DOI: 10.1039/x0xx00000x

www.rsc.org/

The electrochemical properties of graphene are highly sensitive to residual metallic impurities that persist despite various purification efforts. To accurately evaluate the electrochemical performance of graphene, highly purified materials free of metallic impurities are required. In this study, the partial purification of chemically reduced graphene oxides prepared *via* Hummers (CRGO-HU) and Staudenmaier (CRGO-ST) oxidation methods was performed through cyclic voltammetric (CV) scans executed in nitric acid, followed by CV measurements of cumene hydroperoxide (CHP). The purification of graphene was monitored by the changes in the peak current and potential of CHP which is sensitive to iron impurities. The CRGOs were characterized by inductively coupled plasma-mass spectrometry (ICP-MS), electron-dispersive X-ray spectroscopy (EDS), scanning electron microscopy (SEM), X-ray photoelectron spectroscopy (XPS) and CV. The micrographs revealed CRGOs of similar morphologies, but with greater defects in CRGO-HU. The dependences of CHP peak current and peak potential on the number of purification cycles exhibit greater efficiency of removing iron impurities from CRGO-HU than CRGO-ST. This can be attributed to oxidative method that is used in CRGO-HU production, which exposes more defect sites for iron impurities to reside in. This facile electrochemical purification of graphenes can be utilized as routine preparation and cleaning of graphene before electrochemical measurements for analytes that show exceptional sensitivity towards electrocatalytic metallic impurities in sp^2 nanocarbon materials.

Introduction

Graphene, which consists of a single layer of sp^2 carbon atoms packed closely in a honeycomb two-dimensional lattice, has attracted much attention in the field of electrochemistry. As a result of its exceptional electrical conductivity,[1,2] high specific surface area,[3] low cost, rapid heterogeneous electron transfer properties,[2] as well as simple fabrication routes,[4] graphene has been extensively researched in fields of electronic devices,[5-7] batteries,[8,9] solar cells[10] and supercapacitors.[11,12] Amongst the fabrication methods currently available for graphene, the top-down approach is cost effective and has the highest potential to be scaled up for industrial production, and so it is generally the preferred method. This top-down approach involves the chemical oxidation of graphite through the Staudenmaier[13] or Hummers[14] methods, followed by the chemical reduction of the product using reducing agents like hydrazine[15-17] or thermal reduction *via* an exfoliation process.[4,18] It is important to note that the graphite used for the fabrication of reduced graphene oxides, be it natural or synthetic, contains large amounts of metallic impurities, either occurring naturally or unintentionally contaminated as a result of the milling process required to achieve graphite of desired particle sizes.[19]

It was not anticipated that the trace amounts of metallic impurities would have any effect on the electrochemistry of graphene and related sp^2 nanocarbon materials until the study first presented by Compton *et al.*[20] which showed that the apparent electrocatalytic properties of carbon nanotubes (CNTs) towards the redox behaviour of hydrazine was due to residual metallic impurities.[21] Similar findings have been reported for a range of other electrochemically active compounds, such as glucose,[22] hydrogen peroxide,[23] peptides[24] and amino acids.[25] For graphene, the influence of metallic impurities on its electrocatalytic properties has been shown to be significant as well.[26] Subsequently, many groups endeavoured to propose different methods for the purification of various sp^2-carbon (CNTs, graphene) related materials in hopes to attain sufficiently pure materials with electrochemical performance not owing to their impurities. These include thermal treatment in a chlorine atmosphere,[27-31] electrochemical

oxidation coupled with acid washing,[32,33] direct washing of the materials with strong mineral acids, and mechanical cleaning *via* sonication in hydrochloric acid and hydrogen peroxide.[34-36] However, despite the various efforts, these impurities persist and continue to influence the electrochemical properties of the sp^2 nanocarbon materials.[26]

In our previous studies, we have reported that the electrochemical behaviour of organic peroxides with different substituent groups, including cumene hydroperoxide (CHP), is affected by the metallic impurities within CNTs[37] and graphene.[26] It was discussed that the iron oxide nanoparticles within CNTs and chemically modified graphene oxides are responsible for this behaviour. Herein, we will investigate the efficiency of electrochemical purification of chemically reduced graphene oxides, with regards to iron impurities, produced by either the Hummers or Staudenmaier oxidation methods. Inductively coupled plasma-mass spectrometry (ICP-MS), electron-dispersive X-ray spectroscopy (EDS), scanning electron microscopy (SEM), X-ray photoelectron spectroscopy (XPS) and cyclic voltammetry (CV) have been employed to study the effects of electrochemical purification on the materials. In particular, we will show that the iron impurities which are electrocatalytic towards CHP reduction are more accessible to redox activity on chemically reduced graphene oxide produced *via* Hummers method, hence resulting in more efficient electrochemical purification of such graphenes.

Results and Discussion

Electrochemical purification of graphenes using cyclic voltammetry

Graphene has been reported to exhibit excellent heterogeneous electron transfer rate and electrocatalytic activity toward analytes such as CHP. In order for a correct evaluation of the electrochemical performance of graphene, highly purified graphene materials free of metallic impurities are required. Here, we report the partial purification of graphenes *via* a facile electrochemical technique that can be conducted with ease. This electrochemical purification of graphenes provides an additional option of routine preparation and cleaning of graphene before electrochemical measurements.

For electrochemical measurements, the electrodes were prepared according to the protocol that is elaborated in the experimental section. 1 µL aliquot of a dispersed solution (1.0 mg mL^{-1}) of the chemically reduced graphene oxides produced *via* either the Hummers oxidation method (CRGO-HU) or the Staudenmaier oxidation method (CRGO-ST) was drop cast on a freshly polished glassy carbon (GC) electrode and allowed to dry. A CV measurement of CHP (10 mM) in phosphate buffer solution (PBS, 50 mM, pH 7.2) was performed on the unpurified materials (CV denoted as "as-received"). After which, the electrodes were washed gently with deionised water, followed by electrochemical oxidation in nitric acid solution (10 mM), using cyclic voltammetric waveform, with a potential range from -0.5 V to +1.0 V (below the onset of CRGO oxidation, as observed from the CVs of the electrochemical purification step (data not shown)), for 2 cycles at 100 mV s^{-1}. Nitric acid was employed for the electrochemical purification step due to its ability to remove iron impurities from other sp^2 nanocarbon materials, as shown in the study by Heras *et al.*[32] Subsequently, the electrodes were washed gently with deionised water, and a second CV measurement of the CHP probe was conducted to give the CV of CHP on the various materials after 2 cycles of purification (CV denoted as "2x"). This is followed by repeated successive steps of washing, purifying and measuring to give subsequent CVs for the materials after 4, 6, 8 and 10 cycles of purification.

Prior to the electrochemical measurements (as discussed in the later section), CV was performed in a solution of CHP (10 mM) in PBS (50 mM, pH 7.2) on both CRGO-HU and CRGO-ST to establish the maximum number of purification cycles required for the electrochemical oxidation (purification) step. Fig. 1 shows the CVs recorded for CRGO-HU and CRGO-ST in the presence of CHP probe after 0, 5 and 10 cycles of electrochemical purification. It can be observed that after 5 cycles the peak currents of both materials decreased significantly while after 10 cycles, there is only a slight reduction in peak heights. Hence, subsequent CV measurements were recorded up to 10 purification cycles.

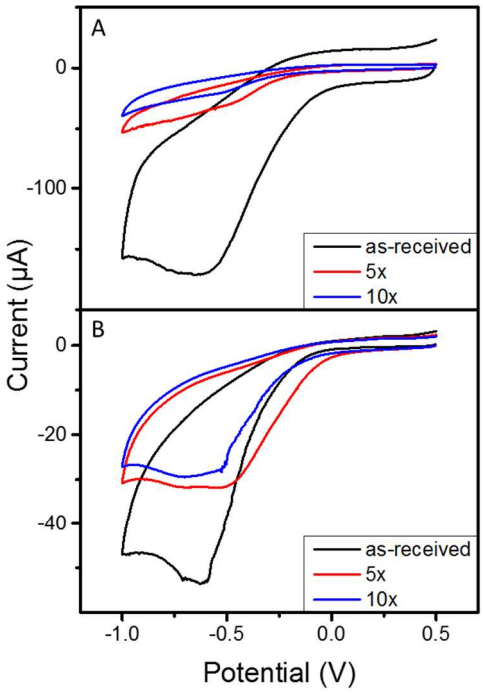

Fig. 1 CVs measured in the presence of 10 mM CHP in 50 mM PBS (pH 7.2) on chemically reduced graphene oxide obtained from graphite oxide prepared by Hummers (CRGO-HU) (A) and Staudenmaier (CRGO-ST) (B) oxidation methods, before purification (black), after 5 cycles (red) and 10 cycles (blue) of purification in 10 mM HNO_3. Scan rate: 100 mVs^{-1}.

In addition, CV scans in CHP probe on glassy carbon (GC) electrode were also conducted (Fig. 2). From the CVs recorded, the GC electrode gave a much smaller peak height and more negative peak potential as compared to CRGO-HU and CRGO-ST. Therefore, it can be concluded that the signals of the CRGO-modified GC electrodes did not originate from the underlying GC electrode.

As mentioned before, CHP has been previously reported to be catalysed by iron impurities in the form of iron oxide (Fe_3O_4) nanoparticles present in chemically reduced graphene oxide.[26] Here, we performed CVs on the CRGOs, together with Fe_3O_4 and iron nanoparticles (FeNPs) over 10 purification cycles to verify the iron species present in the CRGOs that are electrocatalytic towards CHP, and the CV measurements are shown in Fig. 3. The vertical black and grey dashed lines indicate the reduction peak potential of Fe_3O_4 and FeNP respectively. After purification, the peak potentials are expected to increase as the purification step strips away the iron impurities that are electrocatalytic towards the CHP reduction. From Fig. 3, it is observed that the peak potentials of Fe_3O_4, before (dashed) and after (solid) purification, lie closest to those of the CRGO materials while those of FeNP are much more negative than the other materials. Thus, these results affirm that Fe_3O_4 nanoparticles are the main iron species in the CRGOs that catalyse the reduction of CHP.

To verify that the decrease in the peak current of CVs obtained from purification is not due to passivation of the electrode surface, we performed 10 purification cycles in nitric acid solution (10 mM), followed 10 consecutive CVs on CRGO-HU and CRGO-ST modified GC electrodes in the presence of CHP probe (10 mM) in PBS (50 mM, pH 7.2) and the CVs obtained are shown in Fig. 4. There is a significant drop in peak current from the first to second scan, which is characteristic of the occurrence of passivation.

Fig. 5A and 5B represent the dependence of reduction current of the passivation CV scans on number of passivation cycles, and the dependence of reduction current of the CV scans, conducted after various cycles of purification (discussed later), on number of purification cycles for both CRGO-HU and CRGO-ST. Comparing the dependence on number of purification cycles with that on number of passivation cycles illustrates that CRGO-HU exhibits a much steeper decline in peak current after 10 purification cycles (-113 μA) compared to after 10 passivation cycles (-19 μA). On the other hand, CRGO-ST displays a less significant reduction in peak current after 10 purification cycles (-4.6 μA) compared to CRGO-HU but it is still twice that obtained for the corresponding passivation tests (-2.4 μA). Fig. 5C and 5D show the dependence of CHP peak potential on respective number of passivation or purification cycles for both CRGOs. This dependence shows that the changes in CHP reduction potential to substantially more negative potentials are larger after 10 purification cycles (-0.2 V for CRGO-HU and -0.12 V for CRGO-ST), but less so after 10 passivation cycles (-0.01 V for CRGO-HU and -0.03 V for CRGO-ST). These results, coupled with the observation that the onset potentials of the passivation CVs do not vary with the number of CVs performed, led to the conclusion that passivation plays a minor role in the CVs obtained after purification cycles, and the reduction in current and increasingly negative potential of the CHP reduction peak are due to the partial removal of redox-accessible iron impurities.

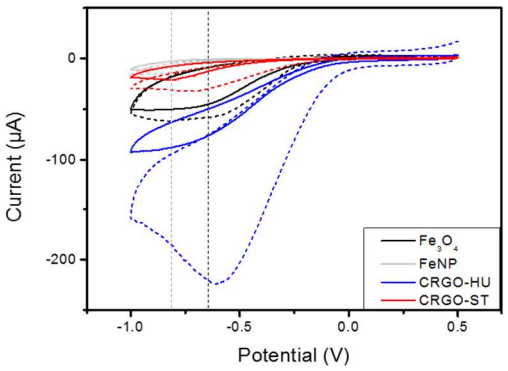

Fig. 3 CVs measured in the presence of 10 mM CHP in 50 mM PBS (pH 7.2) on iron oxide nanoparticles (Fe_3O_4) (black), iron nanoparticles (FeNP) (grey) and chemically reduced graphene oxide obtained from graphite oxide prepared by Hummers (CRGO-HU) (blue) and Staudenmaier (CRGO-ST) (red) oxidation methods, before purification (dashed), and after 10 cycles of purification in 10 mM HNO_3 (solid). Scan rate: 100 mVs^{-1}.

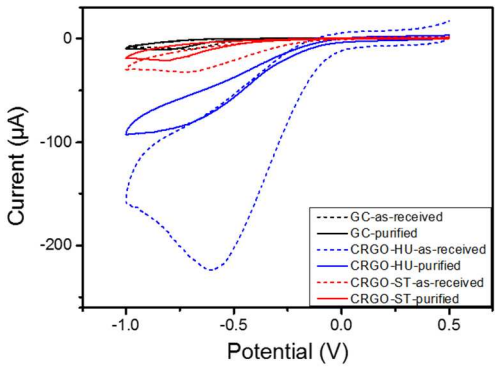

Fig. 2 CVs measured in the presence of 10 mM CHP in 50 mM PBS (pH 7.2) on glassy carbon (GC) (black), chemically reduced graphene oxide obtained from graphite oxide prepared by Hummers (CRGO-HU) (blue) and Staudenmaier (CRGO-ST) (red) oxidation methods, before purification (dashed), and after 10 cycles of purification in 10 mM HNO_3 (solid). Scan rate: 100 mVs^{-1}.

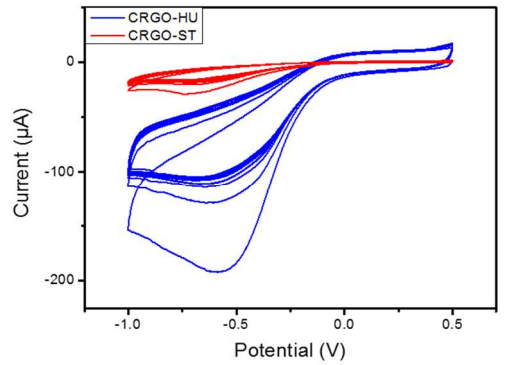

Fig. 4 Ten consecutive CVs measured in the presence of 10 mM CHP in 50 mM PBS (pH 7.2) on chemically reduced graphene oxide obtained from graphite oxide prepared by Hummers (CRGO-HU) (blue) and Staudenmaier (CRGO-ST) (red) oxidation methods, after 10 cycles of purification in 10 mM HNO_3. Scan rate: 100 mVs^{-1}.

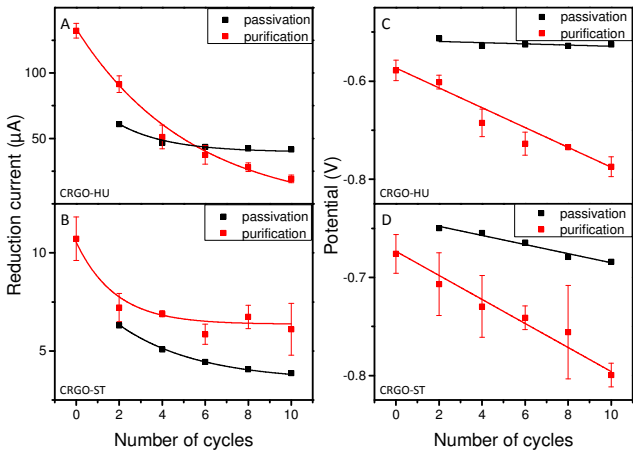

Fig. 5 Dependences of reduction current (A and B) and peak potential (C and D) of CHP on number of cycles of purification in HNO_3 (red) or on number of cyclic voltammetric scans in CHP (black) of chemically reduced graphene oxide obtained from graphite oxide prepared by Hummers (CRGO-HU) and Staudenmaier (CRGO-ST) oxidation methods. Error bars represent triplicate measurements.

The electrochemical purification step involves performing CVs in nitric acid electrolyte. As such, negative control experiments have been carried out to confirm the utility of HNO_3 as the electrolyte for purification, and the dependence(s) of reduction current (and potential) of CHP reduction on the number of cycles of purification in HNO_3 and PBS (pH 7.2) for both CRGO materials are plotted in Fig. 6. Both electrolytes gave decreasing trends for the reduction current. However, HNO_3 demonstrates a steadily decreasing trend for peak potential, while PBS exhibits lower consistency and higher standard deviations for its potential trend. Thus, combining the results for both current and potential, it is acknowledged that HNO_3 displays an advantage over PBS as the electrolyte for the purification step. It should be highlighted here that reduced electrocatalytic effect generally results into shift of peak potentials, which is exactly the case of electrochemically (in HNO_3 environment) purified graphene.

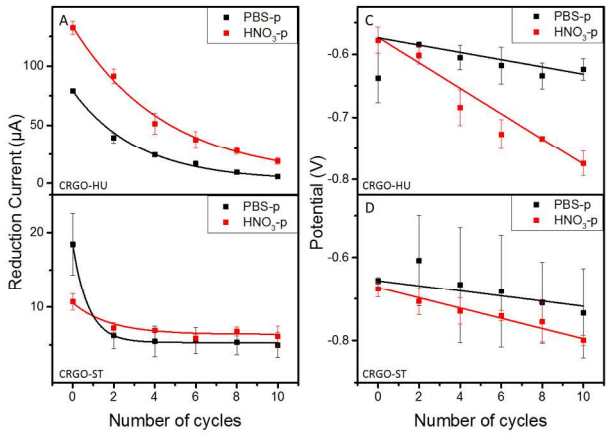

Fig. 6 Dependences of reduction current (A and B) and peak potential (C and D) of CHP on number of cycles of purification in HNO_3 (red) or PBS (pH 7.2) (black) of chemically reduced graphene oxide obtained from graphite oxide prepared by Hummers (CRGO-HU) and Staudenmaier (CRGO-ST) oxidation methods. Error bars represent triplicate measurements.

Redox accessibility of iron impurities affecting efficiency of electrochemical purification

In order to perform the removal of iron impurities from CRGO-HU and CRGO-ST, we must first quantify the amount of said impurities in the respective CRGOs. Using ICP-MS, we examined the iron impurities content in both CRGOs and their concentrations were calculated. In addition, EDS was also performed to complement ICP-MS and the results can be found in Table 1. From the ICP-MS results, it can be observed that CRGO-ST contains 1690 ppm of iron impurities, which is twice as much as CRGO-HU (860 ppm), while the EDS spectra (Table 1) indicate the presence of Fe impurities only in CRGO-HU and the amount present on CRGO-ST was below detection limit. The EDS mappings for CRGO-HU and purified CRGO-HU (CRGO-HU-p) (Fig. 7) show that the iron impurities exist as clusters. This corresponds to a previous study which discovered that metallic impurities in graphene tend to form clusters or nanocrystals.[38]

Similar to the EDS results, the surface sensitive technique XPS have been executed and the wide scan spectra (Fig. 8) did not detect the presence of any Fe in both materials as well. The chlorine 2p peak is presumed to originate from the utilisation of screen printed electrodes (SPE), as a similar peak was also obtained in another study using SPE.[39] The iron species in the CRGOs and purified CRGOs are dispersed throughout and are

Table 1 Quantitative comparison of atomic compositions (% at.) obtained from energy-dispersive X-ray spectra for chemically reduced graphene oxide obtained from graphite oxide prepared by Hummers (CRGO-HU) and Staudenmaier (CRGO-ST) oxidation methods, and the corresponding CRGO materials after 10 cycles of purification in HNO_3 (CRGO-HU-p and CRGO-ST-p). $^{+}$DL denotes detection limit.

Materials	C	O	Fe
CRGO-HU	92.88	5.25	0.04
CRGO-HU-p	88.58	9.73	0.06
CRGO-ST	88.12	8.77	<DL+
CRGO-ST-p	87.03	9.26	<DL+

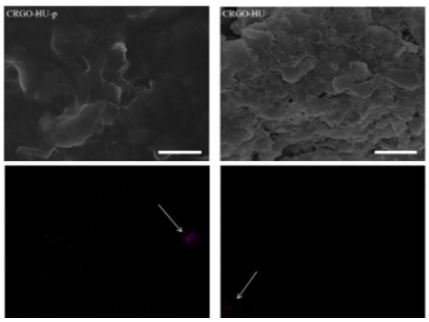

Fig. 7 Scanning electron micrographs (top) of chemically reduced graphene oxides (CRGO) obtained from graphite oxide prepared by Hummers (CRGO-HU) method and the corresponding CRGO after 10 cycles of purification in HNO_3 (CRGO-HU-p) at 2500× magnification and EDS mappings (bottom) of the respective materials. The arrows indicate the iron impurities existing as nanoclusters. Scale bar is 10 μm.

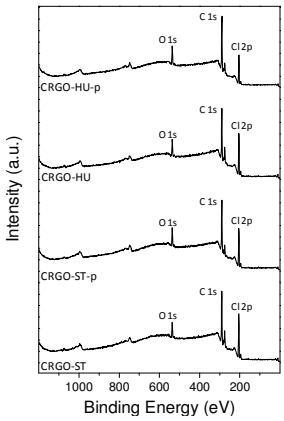

Fig. 8 Wide scan X-ray photoelectron (XPS) spectra of chemically reduced graphene oxide obtained from graphite oxide prepared by Hummers (CRGO-HU) and Staudenmaier (CRGO-ST) oxidation methods, and the corresponding CRGO materials after 10 cycles of purification in HNO_3 (CRGO-HU-p and CRGO-ST-p).

below the detection limits of both EDS and XPS techniques which are *ca.* 0.1% wt. Note that levels observed in SEM/EDX are at limit of the detection of the system and that the Fe impurities are distributed in the sample non-homogenously. This is in good agreement with a previous study where it was found that apparently "pure" CNTs, as determined by EDS and XPS, contained significant amounts of impurities.[40] In order to have insight on the changes of the graphene materials induced by electrochemical purification, we recorded high resolution (HR) XPS of C1s peak. From Figure S-1 (ESI) it can be observed that there is slight decrease of C-O bonds presented in the purified sample and increase of C=O bonds in the same; this is correct for both materials.

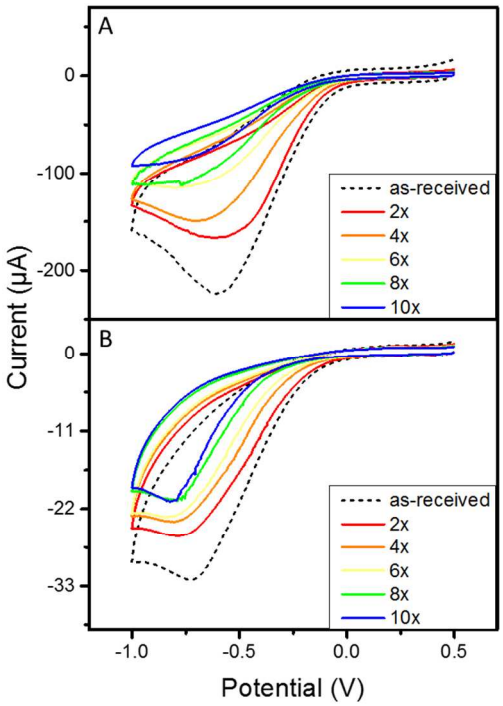

Fig. 9 CVs measured in the presence of 10 mM CHP in 50 mM PBS (pH 7.2) on chemically reduced graphene oxide obtained from graphite oxide prepared by Hummers (CRGO-HU) (A) and Staudenmaier (CRGO-ST) (B) oxidation methods, before purification (dashed), and after various cycles of purification in 10 mM HNO_3. Scan rate: 100 mVs^{-1}.

Subsequently, we moved on to investigate the efficiency of electrochemical purification on the two CRGO materials. Fig. 9 portrays the CVs obtained for CRGO-HU and CRGO-ST in the presence of CHP probe (10 mM) in PBS (50 mM, pH 7.2), after 0, 2, 4, 6, 8 and 10 cycles of purification in nitric acid (10 mM). An analysis of the CVs obtained in Fig. 9 provide dependences of both peak current and potential on number of purification cycles which are illustrated in Fig. 10. Both CRGO-HU and CRGO-ST show decreasing trend in reduction current and potential, though CRGO-HU gave steeper decline for both. The declining peak current and increasingly negative peak potential are the result of the partial removal of redox-accessible iron impurities which are electrocatalytic towards CHP. Furthermore, from Fig. 9, it can be observed that the onset potential of the CVs becomes progressively more negative with increasing number of purification cycles, which signifies that the amount of catalytic iron species in the CRGOs has decreased. Hence, it can be concluded that iron impurities have been successfully removed from the graphene materials. As illustrated in Fig. 10, the steeper decrease in both peak current and potential for CRGO-HU indicate the greater efficiency of electrochemical purification and greater ease of removal of iron impurities from CRGO-HU than CRGO-ST. Hence, it can be deduced that the iron impurities which are electrocatalytic towards CHP reduction are more accessible to redox activity on

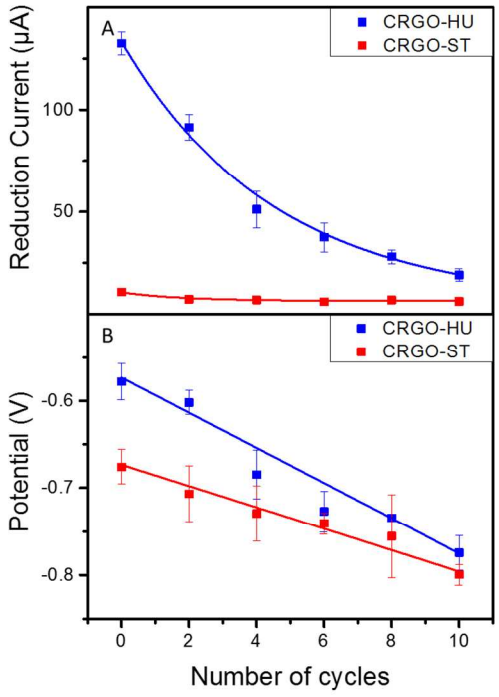

Fig. 10 Dependences of reduction current (A) and peak potential (B) of CHP against number of cycles of purification in HNO_3 of chemically reduced graphene oxide obtained from graphite oxide prepared by Hummers (CRGO-HU) (blue) and Staudenmaier (CRGO-ST) (red) oxidation methods. Error bars represent triplicate measurements.

CRGO-HU, thus resulting in more efficient electrochemical purification of such graphenes. Both CRGOs are produced from natural graphite which contains high amount of iron impurities, as reported previously.[26] Differences in the redox accessibility of the impurities can be attributed to the use of strong oxidant potassium permanganate in the Hummers method, which has been reported to be harsher than the potassium chlorate used in the Staudenmaier oxidation method and leads to more defects.[41] Novoselov *et al.* have shown that metallic impurities tend to form clusters which occupy defect sites.[42] This is evident in Fig. 11 which depicts the SEM images of CRGO-HU and CRGO-ST, imaged at several magnifications, ranging from 370 × to 50 000 ×. The micrographs show that both materials possess similar morphologies, but CRGO-HU exhibits greater defects at the edges.

Conclusion

In summary, we have demonstrated the partial removal of redox-available iron impurities from CRGOs obtained from graphite oxides prepared by the Hummers and Staudenmaier oxidation methods *via* electrochemical purification by examining the reduction potential and current on the number of purification cycles peak signals from the CHP probe which is sensitive to the catalytic properties of iron impurities. The dependences of peak indicate the greater efficiency of the removal of iron impurities from CRGO-HU as compared to CRGO-ST. From the SEM results, we concluded that this superior efficiency of the removal of iron impurities from CRGO-HU is likely due to the harsher Hummers oxidation method which results in higher defects and possibly more sites for clusters of iron impurities to occupy. The current method, which can be conducted with ease, offers an additional option of routine cleaning and preparation of graphene before electrochemical measurements. Further studies can examine the extension of this purification method to other types of graphene materials. To avoid possible contaminations during preparation, it could be considered electrochemical reduction of graphene oxide as preparation method to minimize level of impurities and to create more uniform reduced graphenes.

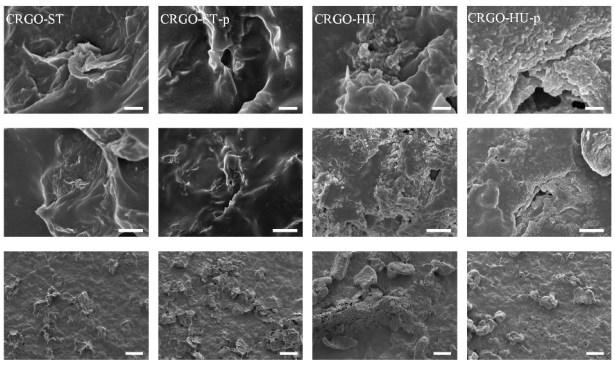

Fig. 11 Scanning electron micrographs of chemically reduced graphene oxides (CRGO) obtained from graphite oxides prepared by Hummers (CRGO-HU) and Staudenmaier (CRGO-ST) oxidation methods, and the corresponding CRGO materials after 10 cycles of purification in HNO_3 (CRGO-HU-p and CRGO-ST-p) at various magnifications. Scale bars are 500 nm (top), 2 μm (middle) and 50 μm (bottom).

Experimental and Methods

Materials and Apparatus

Iron oxide nanoparticles, *N,N*-dimethylformamide, sodium tetraborate decahydrate, potassium phosphate dibasic, sodium phosphate monobasic, sodium chloride, and potassium chloride were purchased from Sigma-Aldrich. Cumene hydroperoxide and iron nanoparticles were obtained from Alfar Aesar and NANO IRON, Czech Republic respectively. Hydrochloric acid, sulphuric acid, potassium permanganate and potassium chlorate were obtained from PENTA, Czech Republic and argon gas was obtained from SIAD. Ultrapure nitric acid and fuming nitric acid (> 90%) were purchased from J. T. Baker. Natural graphite was kindly donated by Asbury Carbons (Asbury, NJ). The screen printed electrodes, glassy carbon electrodes, Ag/AgCl electrode and platinum electrode were purchased from CH Instruments. Deionised water with a resistivity of 18.2 MΩ cm was utilized in the preparation of solutions. Electrochemical experiments using the cyclic voltammetric technique were performed with a μAutolab Type III electrochemical analyser (Eco Chemie, The Netherlands) controlled by the software NOVA 1.8 (Eco Chemie). XPS measurements were carried out with a conventional non-monochromated X-ray source using the Mg Kα line (SPECS XR50, $h\upsilon$ = 1253 eV, 200 W) and a multichannel energy analyser (SPECS Phoibos 100 MCD-5). SEM executed with a JEOL 7600F field- emission SEM (JEOL, Japan), at an acceleration voltage of 5 kV. EDS was conducted at a higher acceleration voltage of 20 kV. The CRGO materials investigated were affixed on an aluminium sample stub using conductive carbon tape for imaging. To reduce charging effect, the prepared sample stubs were sputter-coated with platinum. For XPS, SEM and EDS, the electrochemically purified samples were obtained *via* electrochemical purifications performed on SPE. Inductively coupled plasma-mass spectrometry (ICP-MS) was performed using the Agilent model 7700x ICP-MS, and microwave digestions with ultrapure nitric acid were conducted on the Mars CEM system.

Syntheses of Chemically Modified Graphenes

GRAPHITE OXIDE FROM STAUDENMAIER METHOD (GO-ST)

The graphite oxide that was employed for the synthesis of chemically reduced graphene oxide was prepared from graphite according to the Staudenmaier method.[13] Sulphuric acid (17.5 mL, 95–98%) and nitric acid (9 mL, fuming) were added to a reaction flask at 0 ºC and stirred for 15 min. Graphite (1 g) was then added to the flask and was vigorously stirred to attain a homogeneous dispersion. Subsequently, potassium chlorate (11 g) was added portionwise into the mixture over 15 min to prevent a temperature spike and the formation of explosive chlorine dioxide gas. Upon the dissolution of the potassium chlorate, the mixture was stirred vigorously for 96 h at room temperature, after which the mixture was transferred into deionized water (1 L) and decanted. Graphite oxide was then redispersed and washed repeatedly with hydrochloric acid (5%) solutions to remove sulphate ions, and then washed with deionized water with centrifugation until the pH of the filtrate became neutral. The graphite oxide slurry was then allowed to dry in a vacuum oven at 60 ^{o}C for 48 h before use.

CHEMICALLY REDUCED GRAPHENE OXIDE FROM STAUDENMAIER METHOD (CRGO-ST)

GO-ST (50 mg), synthesized as abovementioned, was dispersed in ultrapure water to form a solution (1.0 mg mL^{-1}) and ultrasonicated (150 W) for 3 h. Hydrazine monohydrate (2 mL) was then added dropwise and the mixture was continuously stirred for 24 h under reflux, after which the reaction mixture was cooled to room temperature and filtered/washed over a PTFE membrane (0.2 µm) with ultrapure water and methanol. CRGO-ST was obtained after drying the mixture at 50 °C for 5 days.

GRAPHITE OXIDE FROM HUMMERS METHOD (GO-HU)

The graphite oxide that was used to synthesize the chemically reduced graphene oxide was prepared from graphite by the modified Hummers method.[14] The graphite particles (0.5 g) were stirred with sulphuric acid (23.0 mL, 95–98 %) at 0 °C for 20 min before the portionwise addition of sodium nitrate (0.5 g) to the mixture. The mixture was then stirred for 1 h and, subsequently, potassium permanganate (3 g) was added portionwise at 0 °C. The mixture was then heated up to 35 °C for 1 h. Water (40 mL) was then added to the mixture which resulted in a temperature rise to 90 °C. This temperature was maintained for 30 min, after which additional water (100 mL) was added into the mixture. Hydrogen peroxide (~10 mL, 30%) was then added dropwise and the warm mixture was centrifuged and washed with warm water. Subsequently, the solid was washed with an abundant volume of water to attain a neutral pH. The material was then dried in a vacuum oven at 30 ^{o}C for 5 days before usage.

CHEMICALLY REDUCED GRAPHENE OXIDE FROM HUMMERS METHOD (CRGO-HU)

GO-HU (100 mg), synthesized by the aforementioned method, was dispersed in ultrapure water to obtain a solution (1.0 mg mL^{-1}) and ultrasonicated (150 W) for 2 h. Hydrazine monohydrate (2 mL) was then added dropwise and the mixture was stirred continuously under reflux for 24 h. Subsequently, the reaction mixture was cooled to room temperature and filtered/washed over a PTFE membrane (0.2 µm) with ultrapure water and methanol. CRGO-HU was obtained after drying the mixture in a vacuum oven at 30 ^{o}C for 5 days.

Preparation of electrodes and electrochemical set-up

The chemically reduced graphene oxide (CRGO-ST and CRGO-HU) and Fe_3O_4 nanoparticles (1.0 mg mL^{-1}) were separately dispersed in *N,N*-dimethylformamide (DMF). Prior to coating, the GC electrode surface was restored to a mirror finish by polishing with 0.05 mm alumina particles on a polishing pad. After 5 min of sonication, 1 µL aliquot of the materials suspension was coated onto a glassy carbon (GC) electrode surface using a micropipette. To obtain a randomly distributed graphene or nanoparticle film on the GC surface, the DMF solvent was allowed to evaporate at room temperature. For the Fe_3O_4 nanoparticles, the deposition step was repeated 4 times to achieve 5 layers of coatings on the GC surface. Cyclic voltammetric measurements were carried out in a 5 mL electrochemical cell at room temperature using a three-electrode configuration consisting of the modified GC working electrode, Ag/AgCl reference electrode and Pt counter electrode. Phosphate buffered solution (PBS) was utilized as the supporting electrolyte for the cumene hydroperoxide (CHP) probe. All CV measurements were carried out at a scan rate of 100 mVs^{-1} and triplicate CV measurements were performed for all materials.

Methodology of electrochemical purification (oxidation)

The electrodes were prepared as mentioned above, followed by a CV measurement of the 10 mM CHP probe in 50 mM PBS (pH 7.2) on the unpurified materials (CV denoted as "as-received"). After which, the electrodes were washed gently with deionised water, followed by electrochemical oxidation in nitric acid solution (10 mM), using cyclic voltammetric waveform, with a potential range from -0.5 V to +1.0 V, for 2 cycles at 100 mV s^{-1}. Subsequently, the electrodes were washed gently with deionised water, and a second CV measurement of the CHP probe was conducted to give the CV of CHP on the various materials after 2 cycles of purification (denoted as "2×"). This is followed by repeated sequential steps of washing, purifying and measuring to give subsequent CVs for the materials after 4, 6, 8 and 10 cycles of purification.

Notes

*Corresponding author
Email: pumera@ntu.edu.sg; pumera.research@outlook.com
Address: School of Physical and Mathematical Science, Division of Chemistry and Biological Chemistry, Nanyang Technological University, 21 Nanyang Link, Singapore.

Supporting Information: XPS and HR-XPS of the materials.

References

1 A. A. Balandin, S. Ghosh, W. Z. Bao, I. Calizo, D. Teweldebrhan, F. Miao and C. N. Lau, *Nano Lett.*, 2008, **8**, 902—907.

2 W. Cai, Y. Zhu, X. Li, R. D. Piner and R. S. Ruoff, *Appl. Phys. Lett.*, 2009, **95**, 123115.

3 M. D. Stoller, S. Park, Y. Zhu, J. An and R. S. Ruoff, *Nano Lett.*, 2008, **8**, 3498—3502.

4 S. Park and R. S. Ruoff, *Nat. Nanotechnol.*, 2009, **4**, 217—224.

5 R. Prasher, *Science*, 2010, **328**, 185—186.

6 R. Sordan, F. Traversi and V. Russo, *Appl. Phys. Lett.*, 2009, **94**, 073305.

7 Y.-M. Lin, C. Dimitrakopoulos, K. A. Jenkins, D. B. Farmer, H.-Y. Chiu, A. Grill and P. Avouris, *Science*, 2010, **327**, 662.

8 E. Yoo, J. Kim, E. Hosono, H.-S. Zhou, T. Kudo and I. Honma, *Nano Lett.*, 2008, **8**, 2277—2282.

9 H. Wang, Y. Yang, Y. Liang, J. T. Robinson, Y. Li, A. Jackson, Y. Cui and H. Dai, *Nano Lett.*, 2011, **11**, 2644—2647.

10 X. Wang, L. Zhi and K. Müllen, *Nano Lett.*, 2008, **8**, 323—327.

11 C. Liu, Z. Yu, D. Neff, A. Zhamu, B. Z. Jang, *Nano Lett.*, 2010, **10**, 4863—4868.

12 Y. Zhu, S. Murali, M. D. Stoller, K. J. Ganesh, W. Cai, P. J. Ferreira, A. Pirkle, R. M. Wallace, K. A. Cychosz, M. Thommes, *Science*, 2011, **332**, 537.

13 L. Staudenmaier, *Ber. Dtsch. Chem. Ges.*, 1898, **31**, 1481—1487.

14 W. S. Hummers, R. E. Offeman, *J. Am. Chem. Soc.*, 1958, **80**, 1339.

15 S. Stankovich, D. A. Dikin, R. D. Piner, K. A. Kohlhaas, A. Kleinhammes, Y. Jia, Y. Wu, S. T. Nguyen, R. S. Ruoff, *Carbon*, 2007, **45**, 1558—1565.

16 H. C. Schniepp, J.-L. Li, M. J. McAllister, H. Sai, M. Herrera-Alonso, D. H. Adamson, R. K. Prud'homme, R. Car, D. A. Saville, I. A. Aksay, *J. Phys. Chem. B*, 2006, **110**, 8535—8539.

17 S. Pei, H. Cheng, *Carbon*, 2012, **50**, 3210—3228.

18 Y. Zhu, S. Murali, W. Cai, X. Li, J. W. Suk, J. R. Potts, R. S. Ruoff, *Adv. Mater.*, 2010, **22**, 3906—3924.

19 H. Marsh, E. A. Heintz and F. Rodríguez-Reinoso, *Introduction to Carbon Technologies*, Universidad de Alicante, Alicante, 1997, p 572.

20 C. E. Banks, A. Crossley, C. Salter, S. J. Wilkins, R. G. Compton, *Angew. Chem. Int. Ed.*, 2006, **45**, 2533—2537.

21 P.-X. Hou, C. Liu, H.-M. Cheng, *Carbon*, 2008, **46**, 2003—2025.

22 C. Batchelor-McAuley, G. G. Wildgoose, R. G. Compton, L. Shao, M. L. H. Green, *Sens. Actuators B*, 2008, **132**, 356—360.

23 B. Šljukić, C. E. Banks, R. G. Compton, *Nano Lett.*, 2006, **6**, 1556—1558.

24 A. Ambrosi, M. Pumera, *Chem. Eur. J.*, 2010, **16**, 1786—1792.

25 M. Pumera, H. Iwai, Y. Miyahara, *Chem. Phys. Chem.*, 2009, **10**, 1770—1773.

26 A. Ambrosi, C. K. Chua, B. Khezri, Z. Sofer, R. D. Webster, M. Pumera, *Proc. Natl. Acad. Sci. U.S.A.*, 2012, **109**, 12899—12904.

27 E. L. K. Chng, H. L. Poh, Z. Sofer, M. Pumera, *Phys. Chem. Chem. Phys.*, 2013, **15**, 5615—5619.

28 *US Pat.* 2914383, November 24, 1959.

29 Graphite Concept Products, Graphitization, *Online Catalog,* 2012, http://www.graphiteconcept.com/content/view/33/27/ (accessed 12/11/13).

30 K. H. Büchel, H. H. Moretto and P. Woditsch, *Industrial Inorganic Chemistry*, Wiley, New York, 2008, p 511.

31 C. J. Im, T. Durney, M. L. Matuszak, *Fuel Process. Technol.*, 1993, **33**, 49—60.

32 A. Heras, A. Colina, J. López-Palacios, P. Ayala, J. Sainio, V. Ruiz, E. I. Kauppinen, *Electrochem. Commun.*, 2009, **11**, 1535—1538.

33 H.-T. Fang, C.-G. Liu, C. Liu, F. Li, M. Liu, H.-M. Cheng, *Chem. Mater.*, 2004, **16**, 5744—5750.

34 E. Dujardin, T. W. Ebbesen, A. Krishnan, M. M. Treacy, J. *Adv. Mater.*, 1998, **10**, 611—613.

35 A. G. Rinzler, J. Liu, H. Dai, P. Nikolaev, C. B. Huffman, F. J. Rodríguez-Macías, P. J. Boul, A. H. Lu, D. Heymann, D. T. Colbert, R. S. Lee, J. E. Fischer, A. M. Rao, P. C. Eklund, R. E. Smalley, *Appl. Phys. A*, 1998, **67**, 29—37.

36 Y. Wang, H. Shan, R. H. Hauge, M. Pasquali, R. E. Smalley, *J. Phys. Chem. B*, 2007, **111**, 1249—1252.

37 E. J. E. Stuart, M. Pumera, *J. Phys. Chem. C*, 2010, **114**, 21296—21298.

38 A. V. Krasheninnikov, P. O. Lehtinen, A. S. Foster, P. Pyykkö, R. M. Nieminen, *Phys. Rev. Lett.*, 2009, **102**, 126807.

39 C. S. Lim, C. K. Chua, M. Pumera, submitted.

40 T. Kolodiazhnyi, M. Pumera, *Small*, 2008, **4**, 1476—1484.

41 H. L. Poh, F. Šaněk, A. Ambrosi, G. Zhao, Z. Sofer, M. Pumera, *Nanoscale*, 2012, **4**, 3515—3522.

42 R. Zan, U. Bangert, Q. Ramasse, K. S. Novoselov, *Nano Lett.*, 2011, **11**, 1087—1092.